

A763

Geo 939 36

prelim

Late Quaternary glacial history and short-term ice-rafted debris fluctuations along the East Greenland continental margin

RUEDIGER STEIN, SEUNG-IL NAM, HANNES GROBE &
HANS HUBBERTEN

*Alfred-Wegener-Institute for Polar and Marine Research, Columbusstrasse,
27568 Bremerhaven, Germany*

1996

Aug 1025

Abstract: High-resolution stable oxygen and carbon isotope and sedimentological investigations were carried out on four west-east profiles at the East Greenland continental margin between 68° and 75° N. The sediment cores represent distinct glacial/interglacial palaeoclimatic episodes over the past 190 ka. Based on oxygen isotope stratigraphy and AMS ¹⁴C dating, our data can be well correlated with the global climate record. However, there are some excursions from the global climate curve suggesting a local/regional overprint by meltwater events of the Greenland Ice Sheet, especially at the beginning of isotope stage 3 and during Termination I. Distinct high-amplitude variations in supply of ice-rafted debris (IRD) indicate repeated advances and retreats of the Greenland Ice Sheet, causing fluctuations in the massive production and transport of icebergs into the Greenland Sea. During the last 190 ka, a number of IRD peaks appear to be correlated with cooling cycles observed in the GRIP Greenland Ice Core. Drastic events in iceberg discharge along the East Greenland continental margin recurred at very short intervals of 1000–3000 years (i.e. much more frequently than the about 10000 years associated with Heinrich events), suggesting short-term collapses of the Greenland Ice Sheet on these time-scales. These late Weichselian Greenland Ice Sheet oscillations appear to be in phase with those in the Barents Sea area. Maximum flux rates of terrigenous (ice-rafted) material were recorded at the continental slope between about 21 and 16 ka, which may correspond to the maximum (stage 2) extension of glaciers on Greenland. The beginning of Termination I is documented by a distinct shift in the oxygen isotopes and a most prominent decrease in flux of IRD at the continental slope caused by the retreat of continental ice masses.

Sedimentary processes, terrigenous sediment supply and biogenic productivity along the East Greenland continental margin are influenced by fluctuations in the extent of the Greenland Ice Sheet, the extent of sea ice, the rate of drifting icebergs, meltwater input and/or oceanic circulation, i.e. factors which are all assumed to be controlled by climate (Figs 1 and 2). The reconstruction of this environmental history of the East Greenland margin and the correlation between terrestrial and marine records are major objectives of the ESF-PONAM (European Science Foundation-Polar North Atlantic Margins) programme (Elverhøi & Dowdeswell 1991). Terrestrial field work on eastern Greenland (e.g. Hjort 1981; Funder 1989; Möller *et al.* 1991; Funder *et al.* 1994) and numerous investigations performed on marine sediments from the Norwegian-Greenland Sea (e.g. Henrich *et al.* 1989; Gard & Backman 1990; Vogelsang 1990; Koç Karpuz & Jansen 1992; Baumann *et al.* 1993) gave important information about changes in palaeoclimate during the last glacial/interglacial cycles. Only a few palaeoenvironmental studies, however, were performed in the heavily sea ice covered

East Greenland continental margin area (e.g. Marienfeld 1992; Mienert *et al.* 1992; Stein *et al.* 1993; Williams 1993; Nam *et al.* 1995). Transport by icebergs is the main mechanism supplying terrigenous material here. In particular, the occurrence of sand- and gravel-sized particles in marine sediments is assumed to be delivered by both icebergs and sea ice and is generally accepted to be a useful tool for identifying ice-rafted debris (IRD) input and reconstructing the activity of glaciers on land (e.g. Ruddiman 1977; Shackleton *et al.* 1984; Grobe 1987; Spielhagen 1991; Hebbeln *et al.* 1994; Fronval *et al.* 1995). As shown in the example of Fig. 3 the sedimentary records from the profile off Scoresby Sund (cf. Fig. 2) are characterized by high-amplitude variations in IRD, suggesting major short-term variations in glacier extension on Greenland (Nam 1996). The IRD-rich horizons, interpreted as short-lived massive discharges of icebergs, are widespread features in the late Pleistocene North Atlantic and intensely investigated and discussed in the recent publications (e.g. Andrews & Tedesco 1992; Bond *et al.* 1992; Broecker *et al.* 1992; Bond & Lotti 1995). These so-called 'Heinrich layers' or 'Heinrich events'

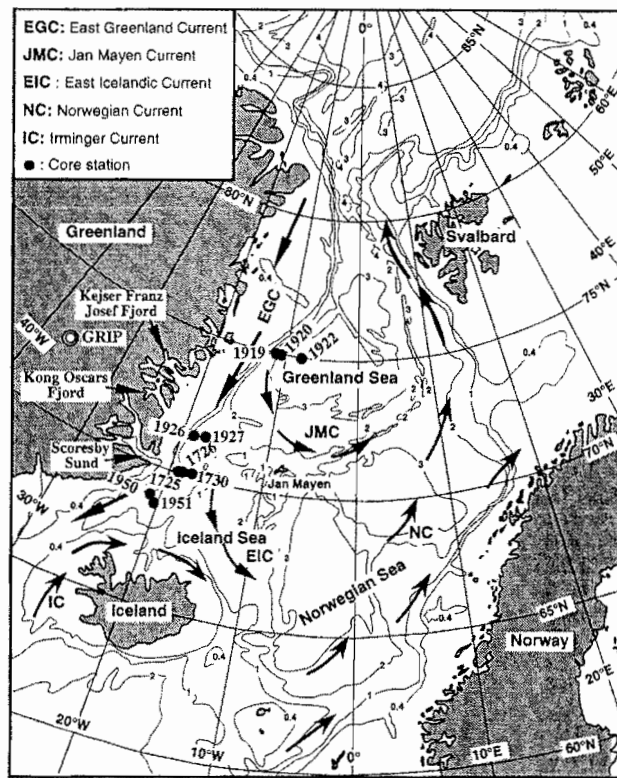


Fig. 1. Bathymetry and major surface water current patterns of the Greenland-Iceland-Norwegian Sea and core locations at the East Greenland continental margin. Bathymetry in 1000 m.

(Heinrich 1988; Broecker *et al.* 1992) occurring every 5–10 ka, are inconsistent with Milankovitch orbital periodicities and their origin is still under discussion (e.g. Bond *et al.* 1992).

In this paper, we concentrate on stable isotope stratigraphy and IRD and its change through

time and space. Major questions to be answered are as follows. Is it possible to link the IRD records with the Greenland Ice Sheet history and the terrestrial climate record? What is the frequency of variability of IRD input? Is it possible to link some of our IRD peaks to

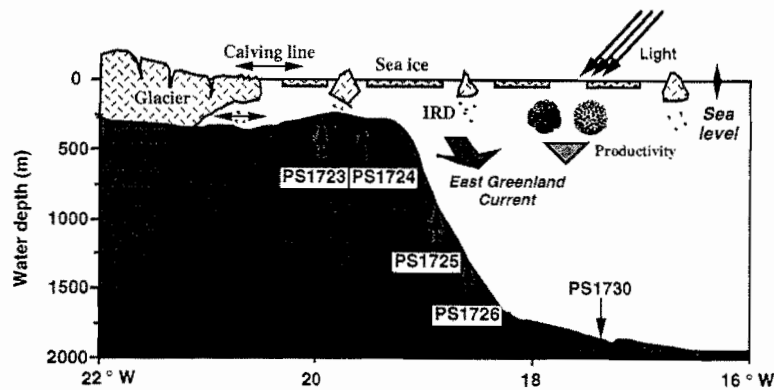


Fig. 2. Simplified scheme of the continental margin profile off Scoresby Sund (cores PS1723–PS1730), indicating the major climatic and oceanographic factors and processes controlling the sedimentation along the East Greenland continental margin.

Fig. 3
10 cm

Hein
corre
Core

Met

Sedi
a dia
cula
betw
expe
and
ing
on
wat
340
sequ
base
top
B
deta
(for
mei
199
deta
for

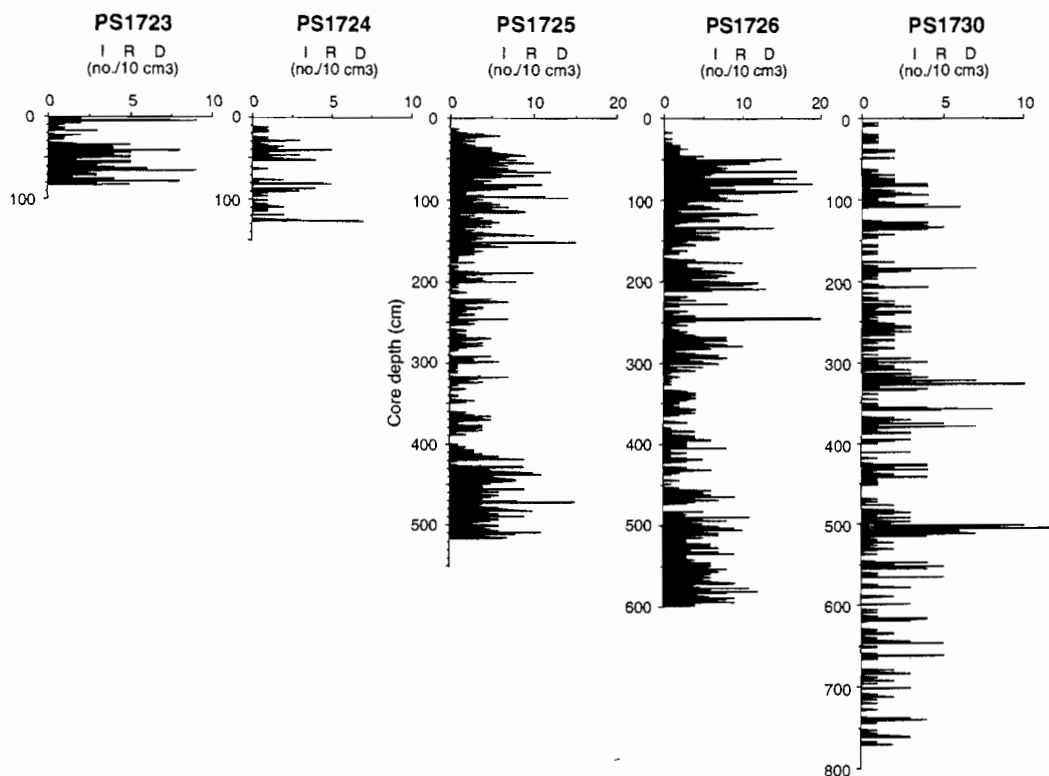


Fig. 3. Distribution of IRD (i.e. gravel fraction >2 mm, counted in X-radiographs and expressed as numbers per 10 cm^3) at cores PS1723–PS1730. For location of profile, see Figs 1 and 2.

Heinrich events? Furthermore, we try to correlate our marine data with the GRIP Ice Core record.

Methods

Sediments were recovered by gravity coring (with a diameter of 12 cm) on four profiles perpendicular to the East Greenland continental margin between about 68° and 75°N during *Polarstern* expeditions ARK-V/3 and ARK-VII/3 in 1988 and 1990, respectively (Fig. 1, Table 1). The coring positions have been carefully selected based on Parasound and Hydrosweep profiling. The water depths of core sites vary between 280 and 3400 m. The age represented in the sedimentary sequences is Late Pleistocene to Holocene as based on AMS ^{14}C dating and oxygen stable isotope records.

Before opening, magnetic susceptibility was determined using a Bartington MS2 core logger (for detailed descriptions of the applied equipment and method, see Nowaczyk 1991; Fütterer 1992). After opening, all cores were described in detail. X-Radiographs were made from all cores for the determination of sedimentary structures.

Coarse-grained detritus >2 mm was counted in 1 cm intervals from the X-radiographs to evaluate the content of IRD (Grobe 1987). The IRD values were smoothed by a five-point moving average.

All cores were routinely sampled at 5–10 cm intervals; additional samples were taken at distinct changes in lithology and/or colour. About 30 cm^3 subsamples were taken for coarse

Table 1. Core number, core length, latitude and longitude and water depth of cores investigated

| Core No. | Core length (cm) | Latitude ($^\circ\text{N}$) | Longitude ($^\circ\text{W}$) | Water depth (m) |
|----------|------------------|-------------------------------|--------------------------------|-----------------|
| PS1919 | 373 | $74^\circ59.8'$ | $11^\circ54.2'$ | 1876 |
| PS1920 | 750 | $74^\circ59.7'$ | $11^\circ04.3'$ | 2717 |
| PS1922 | 493 | $75^\circ00.0'$ | $08^\circ46.3'$ | 3350 |
| PS1926 | 319 | $71^\circ29.6'$ | $18^\circ16.5'$ | 1493 |
| PS1927 | 491 | $71^\circ29.7'$ | $17^\circ07.1'$ | 1734 |
| PS1725 | 516 | $70^\circ06.9'$ | $18^\circ49.9'$ | 879 |
| PS1726 | 600 | $70^\circ07.0'$ | $18^\circ38.9'$ | 1174 |
| PS1730 | 779 | $70^\circ07.2'$ | $17^\circ42.1'$ | 1617 |
| PS1950 | 421 | $68^\circ53.4'$ | $20^\circ55.7'$ | 1480 |
| PS1951 | 789 | $68^\circ50.5'$ | $20^\circ49.2'$ | 1481 |

Table 2. AMS ^{14}C datings of sediment samples from selected core intervals; listed are uncorrected radiocarbon ages and reservoir-corrected (550 years) ages. AAR-1291, AAR-1292, etc. are the sample numbers at the AMS ^{14}C dating laboratory of the Institute of Physics and Astronomy, Aarhus University, Denmark

| Core | Laboratory No | Depth (cm bsf) | Age (years BP) | Reservoir corrected age (years BP) |
|----------|---------------|-------------------|-------------------|---------------------------------------|
| PS1919-2 | AAR-1291 | 7 | 7820 ± 100 | 7270 ± 100 |
| | AAR-1292 | 13 | 16620 ± 180 | 16070 ± 180 |
| | AAR-1293 | 51 | 20050 ± 260 | 19500 ± 260 |
| | AAR-1294 | 100 | 31500 ± 570 | 30950 ± 570 |
| PS1920-1 | AAR-1295 | 6 | 5230 ± 90 | 4680 ± 90 |
| | AAR-1296 | 47 | 17380 ± 180 | 16830 ± 180 |
| | AAR-1297 | 80 | 12050 ± 130 | 11500 ± 130 |
| | AAR-1298 | 144 | 24330 ± 370 | 23780 ± 370 |
| PS1922-1 | AAR-1299 | 156 | 19180 ± 290 | 18630 ± 290 |
| PS1926-1 | AAR-1301 | 1 | 540 ± 110 | -10 ± 110 |
| | AAR-1302 | 32 | 15490 ± 210 | 14940 ± 210 |
| PS1927-2 | AAR-1303 | 8 | 6630 ± 90 | 6080 ± 90 |
| | AAR-1304 | 52 | 13760 ± 170 | 13210 ± 170 |
| | AAR-1305 | 72 | 16620 ± 160 | 16070 ± 160 |
| | AAR-1704 | 100 | 18910 ± 210 | 18360 ± 210 |
| | AAR-1705 | 140 | 21240 ± 250 | 20690 ± 250 |
| | AAR-1306 | 170 | 23230 ± 240 | 22680 ± 240 |
| PS1726-1 | | 40 | Vedde ash | 10600 |
| | AAR-1149 | 60 | 15590 ± 130 | 15040 ± 130 |
| | AAR-1150 | 80 | 18900 ± 170 | 18350 ± 170 |
| | AAR-1701 | 90 | 19950 ± 270 | 19400 ± 270 |
| | AAR-1151 | 120 | 27500 ± 330 | 26950 ± 330 |
| PS1730-2 | AAR-1152 | 20 | 8460 ± 10 | 7910 ± 110 |
| | | 35 | Vedde ash | 10690 |
| | ARR-1153 | 70 | 14870 ± 140 | 14320 ± 140 |
| | AAR-1154 | 80 | 16820 ± 150 | 16270 ± 150 |
| | AAR-1155 | 90 | 19150 ± 190 | 18600 ± 190 |
| | AAR-1156 | 140 | 23550 ± 360 | 23000 ± 360 |
| | AAR-1157 | 160 | 25450 ± 310 | 24900 ± 310 |
| | AAR-1158 | 200 | 28500 ± 650 | 27950 ± 650 |
| | PS1950-2 | AAR-1307 | 58 | 14710 ± 140 |
| PS1951-1 | ARR-1308 | 60 | 15050 ± 130 | 14500 ± 130 |
| | AAR-1309 | 72 | 15840 ± 140 | 15290 ± 140 |
| | ARR-1702 | 83 | 17380 ± 190 | 16830 ± 190 |
| | AAR-1703 | 123 | 19760 ± 240 | 19210 ± 240 |
| | AAR-1310 | 156 | 22060 ± 240 | 21510 ± 240 |

fraction analysis, stable isotopes and ^{14}C dating. Further subsamples were taken for the analysis of grain size distribution, clay mineralogy, carbonate and organic carbon content. The accompanied sedimentological data are presented and discussed in Stein *et al.* (1993), Nam (1996), Nam *et al.* (1995). Flux rates of terrigenous matter were calculated following van Andel *et al.* (1975).

Stable oxygen and carbon isotope records were determined on planktonic foraminiferal tests *N. pachyderma* sin. with 10 specimens per sample of the 125–250 μm fraction, using a Finnigan MAT 251 mass spectrometer. Two

thousand specimens of *N. pachyderma* sin. per sample were selected for AMS ^{14}C dating of the uppermost intervals (Table 2). The dating was performed at the AMS ^{14}C Dating Laboratory of the Institute of Physics and Astronomy, Aarhus University, Denmark.

Results and discussion

Based on the lithological core description, the sediments of all cores investigated are dominantly of terrigenous origin and show distinct

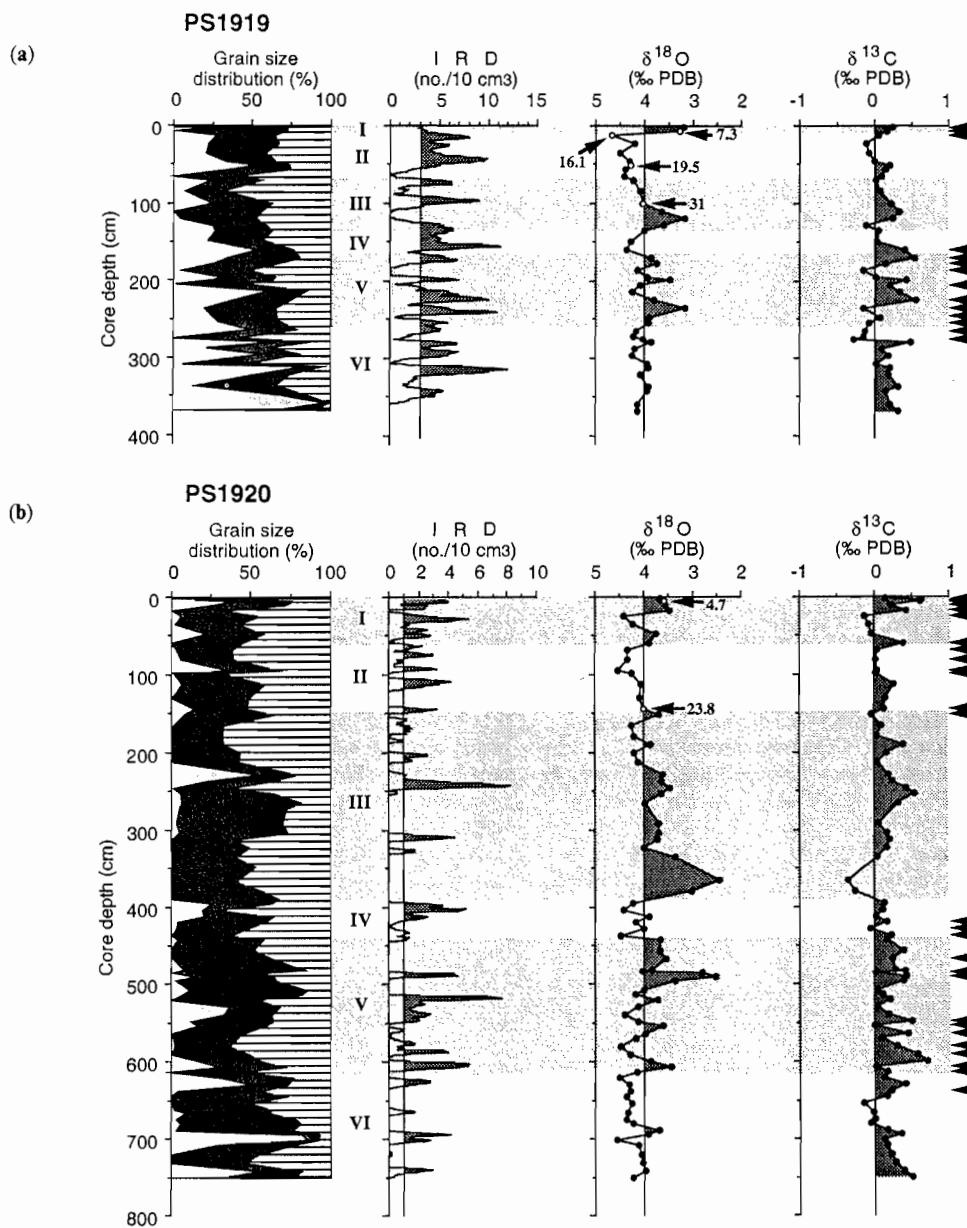


Fig. 4. Records from sediment cores (a) PS1919, (b) PS1920 and (c) PS1922. For all cores, grain-size distributions (sand-silt-clay), the amount of IRD i.e. gravel fraction $>2\text{mm}$, counted in X-radiographs, smoothed by the five-point moving average method, and expressed as numbers per 10cm^3 and stable oxygen and carbon isotope values (measured on the planktonic foraminifer *N. pachyderma* sin.) are shown. Roman numbers indicate oxygen isotope stages. Arrows in the oxygen isotope record and numbers indicate AMS ^{14}C ages (cf. Table 2). Black triangles mark samples in which the benthic foraminifer *C. wuellerstorfi* is present.

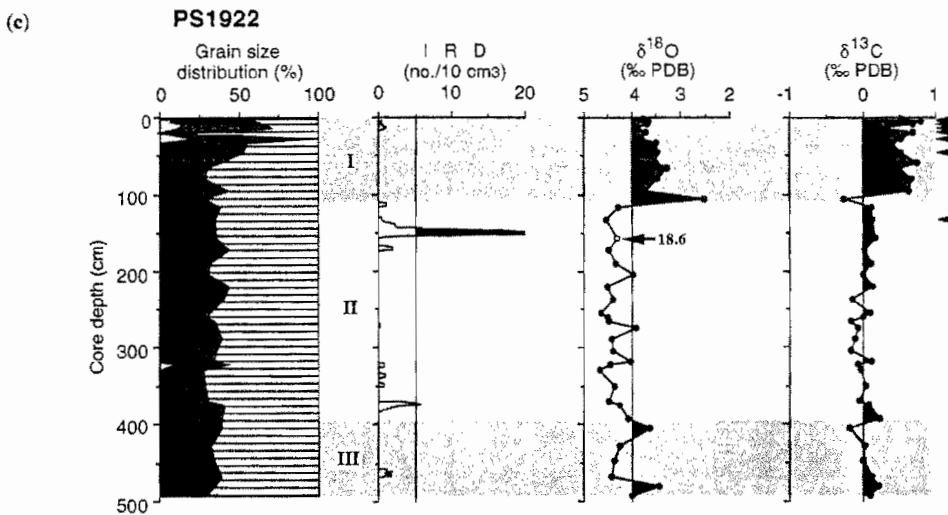


Fig. 4. Continued

variations in sediment colours, sedimentary structures, the abundance of sand-sized siliciclastic components and grain size distribution.

Stable isotope stratigraphy and palaeoenvironment

The results of $\delta^{18}\text{O}$ analyses indicate that the cores contain oxygen isotope stages 1–7 (cores PS1725, PS1726, PS1730), 1–6 (cores PS1919, PS1920, PS1951), 1–5 (core PS1927), 1–3 (core PS1922) and 1–2 (cores PS1926, PS1950) (Figs 4–7). The results of AMS ^{14}C datings (Table 2), the isotope records and the position of the Vedde Ash (see later) suggest that, of the gravity

cores taken, only core PS1926 sampled the sediment–water interface. Based on the comparison of the oxygen isotope values from box core PS1730 taken at the same location as the gravity core PS1730, the uppermost 23 cm are lost from the gravity core (Nam *et al.* 1995).

Oxygen isotope stages 1 and 2 were identified by AMS ^{14}C datings (Table 2) and the occurrence of a prominent ash layer (correlated with the 10.6 ka Vedde ash; Mangerud *et al.* 1984). For the last post-glacial period (Holocene) within cores PS1725 and PS1726, no isotope data was available due to the lack of calcareous foraminiferal tests. Oxygen isotope stage 5 was recognized by the occurrence of the benthic foraminifer species *C. wuellerstorfi* (e.g. Streeter

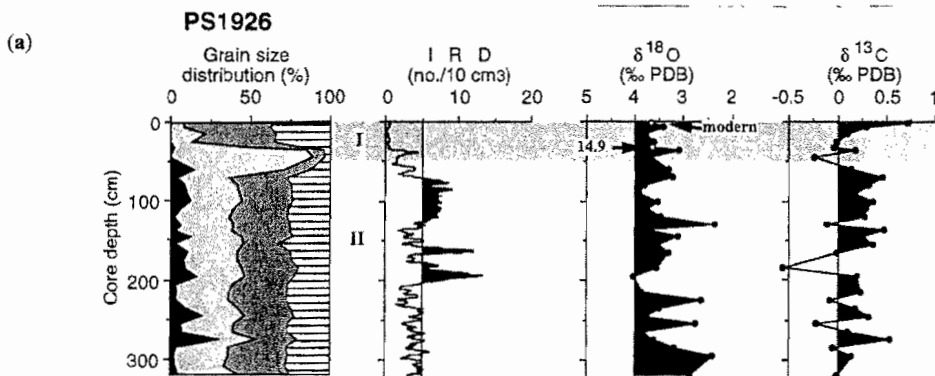


Fig. 5. Records from sediment cores (a) PS1926 and (b) PS1927. For both cores, grain size distributions (gravel–sand–silt–clay), the amount of IRD (i.e. gravel fraction >2 mm, counted in X-radiographs, smoothed by the five-point moving average method and expressed as numbers per 10 cm^3) and stable oxygen and carbon isotope values (measured on the planktonic foraminifer *N. pachyderma* sin.) are shown. Roman numbers indicate oxygen isotope stages. Arrows in the oxygen isotope record and numbers indicate AMS ^{14}C -ages (cf. Table 2). Black triangles mark samples in which the benthic foraminifer *C. wuellerstorfi* is present.

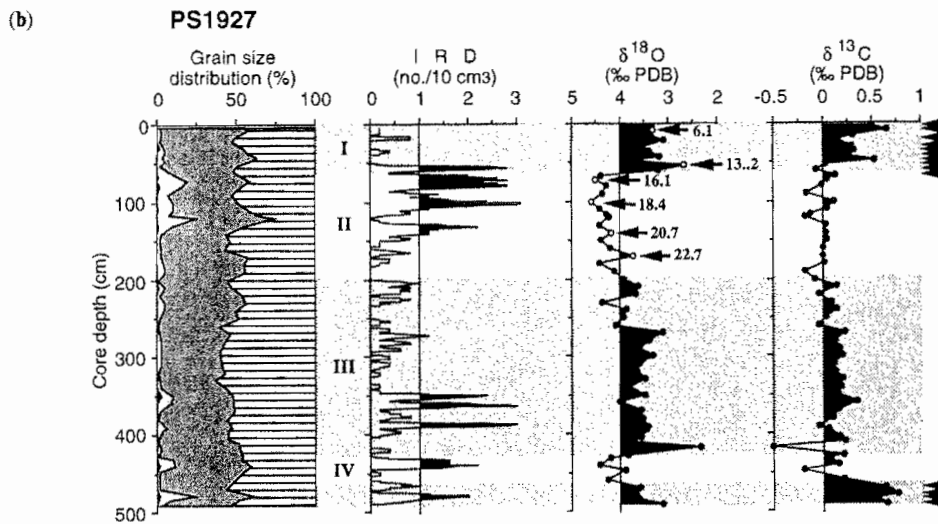


Fig. 5. Continued

et al. 1982; Vogelsang 1990; Jünger 1993). Furthermore, stage 5 is characterized by very heavy carbon isotope values.

The occurrence of a second specific ash layer in cores PS1725, PS1726 and PS1730 at depths of 369, 460 and 730 cm, respectively, was used to identify isotope stage 7 (Fig. 6; Nam *et al.* 1995). Based on the results of major element determinations on volcanic glass particles from the three

cores (Wallrabe-Adams unpublished data), this ash zone can be correlated with other deep-sea cores in the Greenland-Norwegian Sea, where this ash is found within oxygen isotope stage 7 (Sejrup *et al.* 1989; Birgisdottir 1991; Lackschewitz 1991; Baumann *et al.* 1993).

In general, most of the isotope curves resemble the global isotope record (e.g. Shackleton & Opdyke 1973; Martinson *et al.* 1987), with some

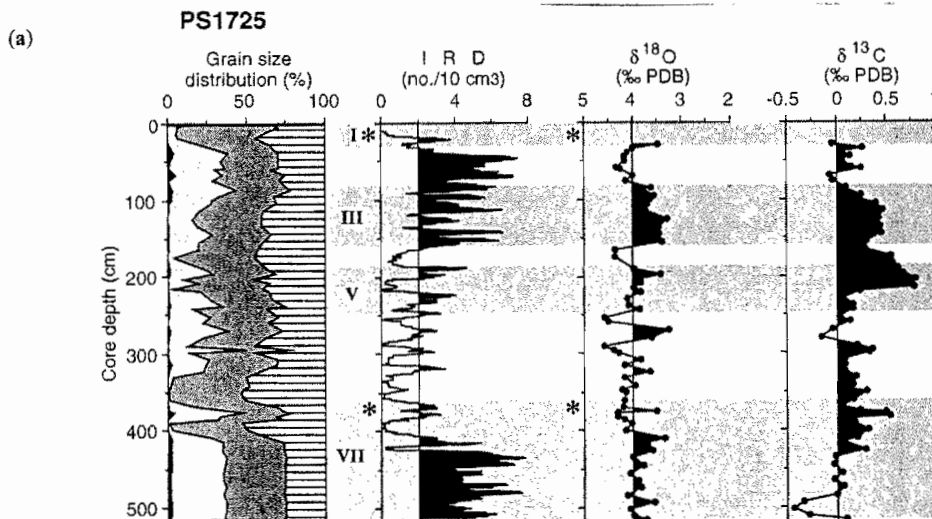


Fig. 6. Records from sediment cores (a) PS1725, (b) PS1726 and (c) PS1730 (deep sea). For all cores, grain size distributions (gravel-sand-silt-clay), the amount of IRD (i.e. gravel fraction >2 mm, counted in X-radiographs, smoothed by the five-point moving average method and expressed as numbers per 10 cm^3) and stable oxygen and carbon isotope values (measured on the planktonic foraminifer *N. pachyderma* sin.) are shown. Roman numbers indicate oxygen isotope stages, asterisks indicate ash layers. Arrows in the oxygen isotope record and numbers indicate AMS ^{14}C -ages (cf. Table 2). Black triangles mark samples in which the benthic foraminifer *C. wuellerstorfi* is present.

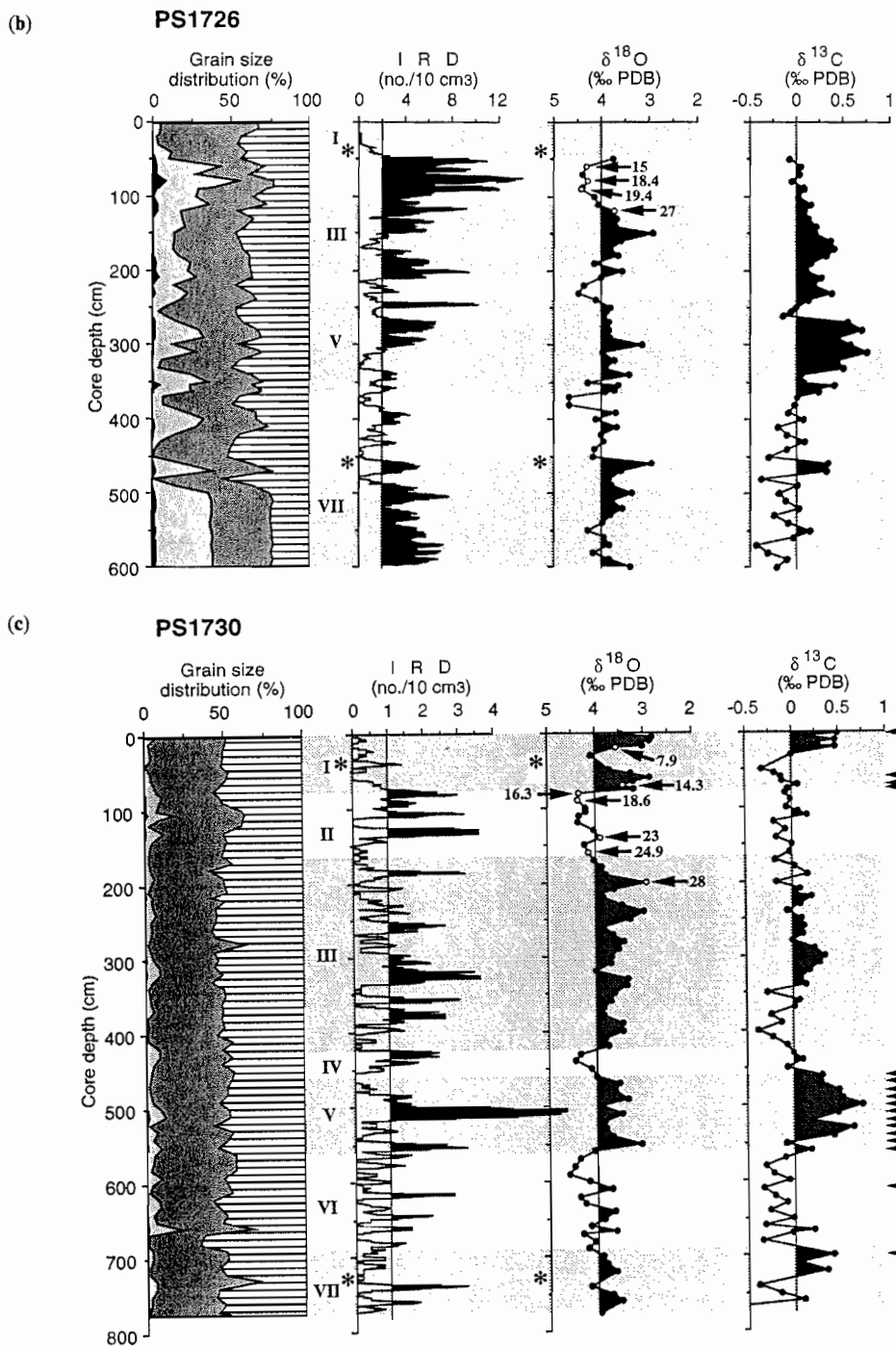


Fig. 6. Continued

excursions to lighter values (Figs 4–7). These lighter values are probably caused by local/regional meltwater supply (cf. Duplessy *et al.* 1991; Sarnthein *et al.* 1992) and are especially seen at the beginning of oxygen isotope stage 3 and during Termination I. Similar deglacial

meltwater anomalies were also recorded in the Norwegian–Greenland Sea and Fram Strait during Termination I (e.g. Jones & Keigwin 1988; Vogelsang 1990; Sarnthein *et al.* 1992) as well as in the central Arctic Ocean (Stein *et al.* 1994a; 1994b).

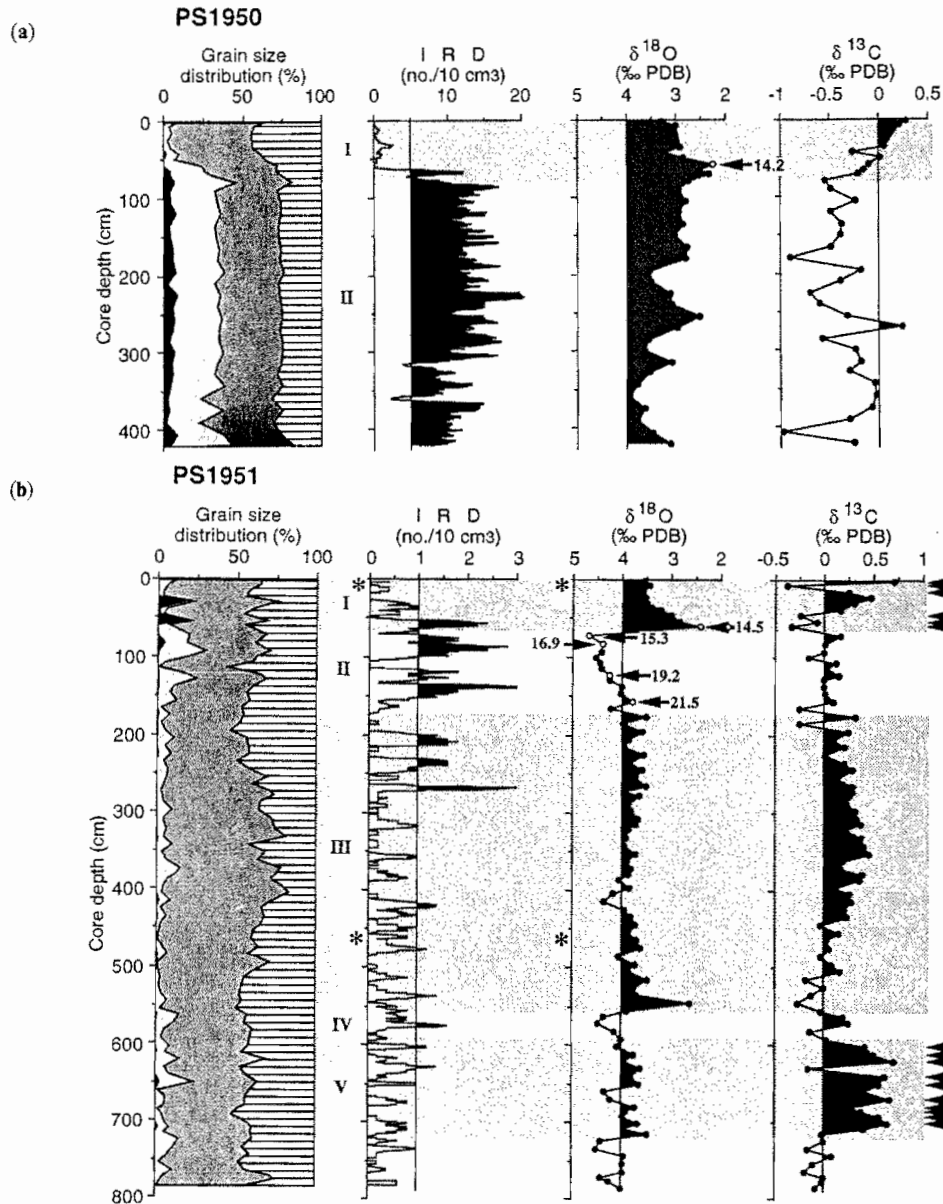


Fig. 7. Records from sediment cores (a) PS1950 and (b) PS1951. For both cores, grain size distributions (gravel-sand-silt-clay), the amount of IRD (i.e. gravel fraction >2 mm, counted in X-radiographs, smoothed by the five-point moving average method and expressed as numbers per 10 cm³) and stable oxygen and carbon isotope values (measured on the planktonic foraminifer *N. pachyderma* sin.) are shown. Roman numbers indicate oxygen isotope stages, asterisks indicate ash layers. Arrows in the oxygen isotope record and numbers indicate AMS ¹⁴C ages (cf. Table 2). Black triangles mark samples in which the benthic foraminifer *C. wuellerstorfi* is present.

During the last deglaciation (Termination I), Last Glacial Maximum (LGM) $\delta^{18}\text{O}$ values of *N. pachyderma* sin. decrease from about 4.5‰ to Holocene values as low as 2.5‰. The c. 2‰ glacial-interglacial shift in $\delta^{18}\text{O}$ exceeds the glacial-interglacial ice-volume effect of about 1.1–1.3‰ (e.g. Chappell & Shackleton 1986; Shackleton 1987; Fairbanks 1989). This isotope shift can be explained either by increasing temperature or decreasing salinity. Because the modern surface water temperature in the East Greenland Current system is approximately -1°C (Gorshkov 1983; Hubberten *et al.* unpublished data), additional cooling during glacial times is unlikely. Thus the excess in $\delta^{18}\text{O}$ was probably caused by decreasing salinity resulting from increased meltwater discharge during the last deglaciation (Termination I).

The $\delta^{18}\text{O}$ records of upper slope cores PS1926 (Fig. 5a) and PS1950 (Fig. 7a) do not follow the global isotope signal. The $\delta^{18}\text{O}$ values from before Termination I (LGM) and after Termination I (Holocene) are similar: around 4–3‰, with minimum values of <3‰. Thus, the LGM oxygen isotope values are 1–1.7‰ lighter than the LGM values of the other cores (4.5‰). This result probably indicates a local meltwater influence present at these two core sites during isotope stage 2. The most probable meltwater source is from advancing glaciers in Scoresby Sund (core PS1950) and Kong-Oscars-Fjord/Kejser-Franz-Josef-Fjord (Fig. 1). This meltwater signal is best developed at core PS1950, where it is reflected in very light oxygen and carbon isotope values that correlate with increased abundances of IRD (Fig. 7a).

Fluctuations in the amount and composition of IRD during isotope stages 1–7 and East Greenland glacial history

The sediment cores from the slope and deep-sea areas off East Greenland (Table 1) mainly show alternating sequences of silty clay and sandy mud with high-amplitude variations of IRD (Figs 4–7). The amount of sand fraction and IRD best documented at the slope cores suggests that several major pulses of glacial activity and supply of terrigenous material by glaciomarine processes occurred during the last 190 ka.

In general, the amount of IRD at the slope cores is significantly higher than at the deep-sea cores. During isotope stages 2, 3, and 6/7, a distinct increase in the amounts of IRD is observed. In most cores, the maximum IRD content was recorded during isotope stage 2

with the absolute maximum at core PS1950. However, pulses of increased amounts of IRD also occur during warm isotope stages. High-amplitude variations of IRD input were recorded in cores PS1919 and PS1730 throughout the last 150 ka (Figs 4a and 6c). At these cores, at least 11 major pulses of increased IRD input occur during isotope stages 5 to 1 (about one event per 11 000 a). This suggests that also during warm stages (such as oxygen isotope stage 5) East Greenland glaciers retreated and advanced and supplied large amounts of IRD into the East Greenland Current system.

The maximum occurrence of IRD in the sedimentary records off Scoresby Sund (cores PS1725 and PS1726; Figs 6a and 6b) is older than isotope stage 6 (i.e. pre-Saalian) and probably corresponds to the pre-Saalian 'Lollandshelv Glaciation' recorded on Jameson Land (Funder *et al.* 1994; Möller *et al.* 1994). During stage 6 when a maximum extension of the East Greenland glaciers occurred (Saalian or 'Scoresby-Sund Glaciation'; Hjort 1981; Funder 1984; Funder *et al.* 1994; Möller *et al.* 1994), the IRD abundances off Scoresby Sund are much lower than those described for the LGM (stage 2). This result suggests that the more extensive continental ice masses on Greenland and sea ice cover in the Greenland Sea during stage 6 (compared with stage 2) prevented the supply and accumulation of IRD at the continental slope off Scoresby Sund (Fig. 6). In the northernmost profile (cores PS1919 and PS1920; Fig. 4) the IRD abundances of the stage 2 and stage 6 intervals are similar. The distinct IRD peak recorded at the well-dated core PS1730 within stage 5 (Fig. 6c) may coincide with the stage 5d or 'Auccelaelv stage' glaciation described in the Scoresby Sund area (Funder *et al.* 1994; Israelson *et al.* 1994).

The time interval of about 74 to 25 ka (i.e. isotope stages 4 and 3) are missing from terrestrial sites. This is explained either by (1) distinctly lowered sea level and, thus, sedimentation below the present sea level and later removal of sediments by glacier erosion or (2) problems of dating existing fluvial and glacial sequences (Funder *et al.* 1994). In the marine records, however, major pulses of IRD are seen, suggesting significant advances and retreats of the inland ice margin during that time interval, i.e. before the last major glacial advance (late Weichselian or 'Flakkerhuk stade'; see later). In the stage 3 interval of core PS1730, maxima (minima) in IRD coincide with heavy (light) $\delta^{18}\text{O}$ values (Fig. 6c), which may reflect short-term climatic cycles ('Dansgaard-Oeschger Cycles'; for detailed discussion see Nam 1996). These results suggest that

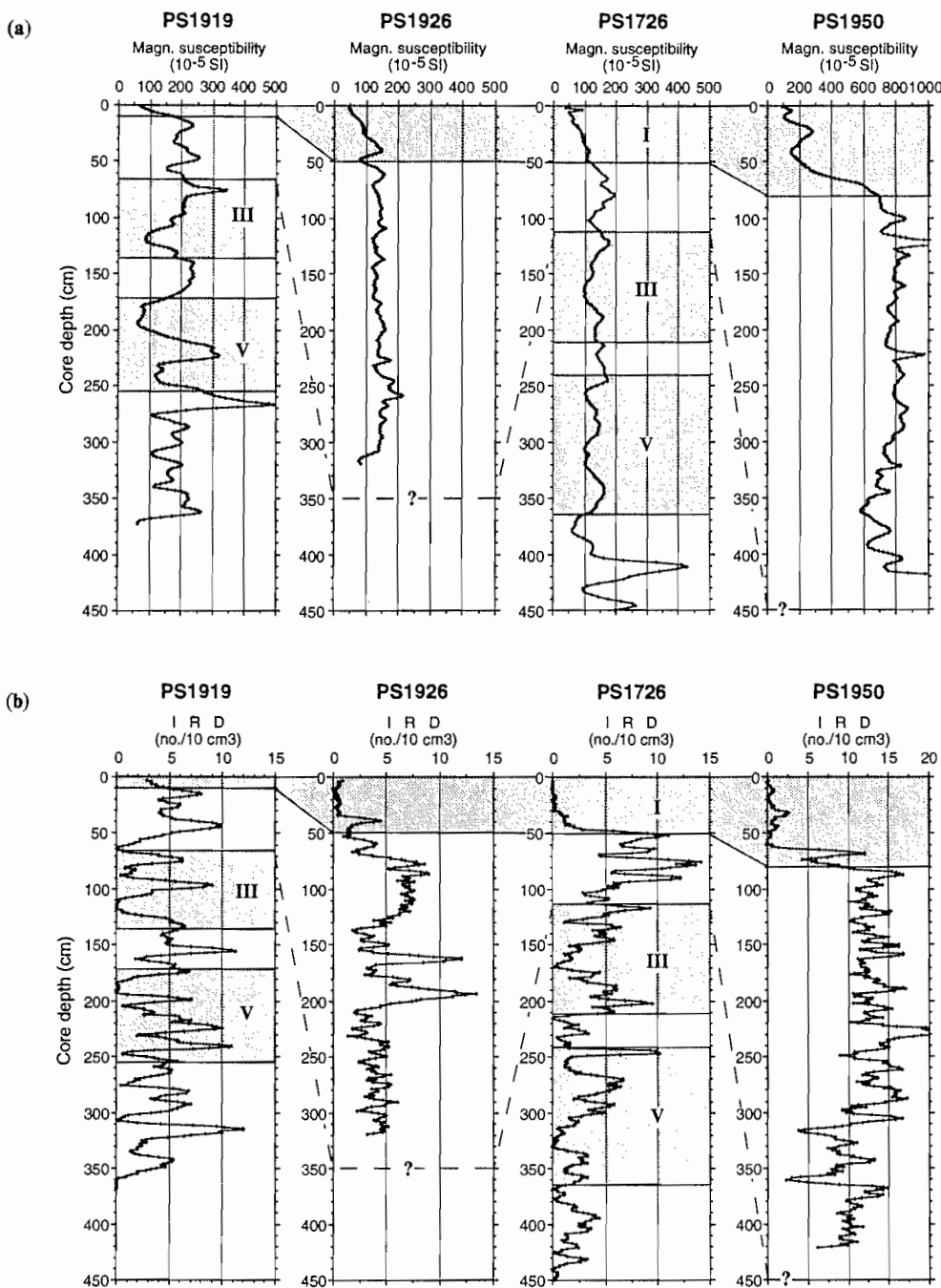


Fig. 8. (a) Magnetic susceptibility values and (b) amount of IRD (i.e. gravel fraction >2mm, counted in X-radiographs, smoothed by the five-point moving average method and expressed as numbers per 10 cm³) at cores PS1919, PS1926, PS1726 and PS1950.

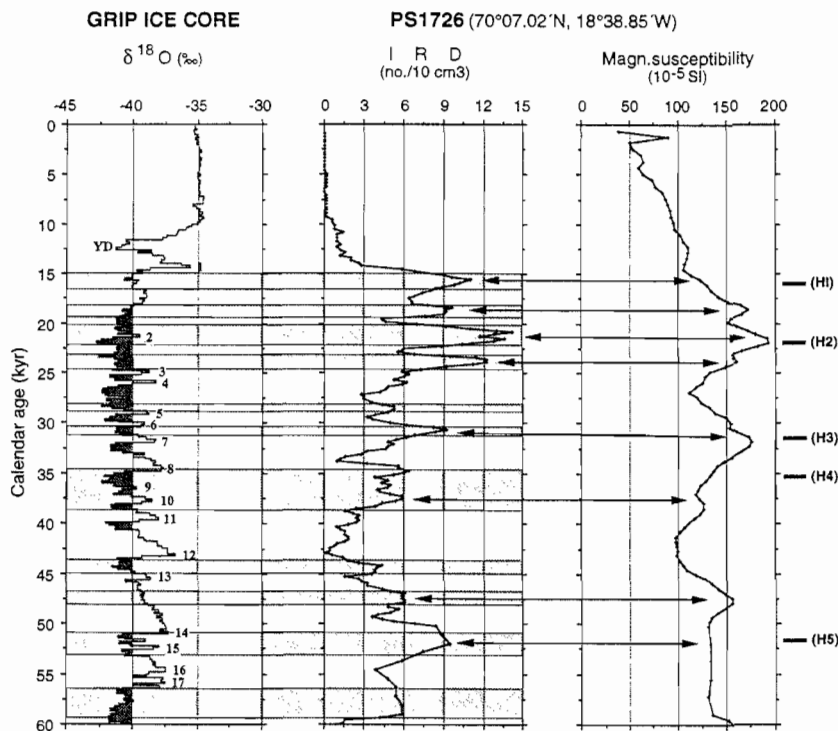


Fig. 9. Correlation between the oxygen isotope record of the GRIP Ice Core (Dansgaard *et al.* 1993) and IRD content and magnetic susceptibility values of core PS1726, plotted versus calendar years. For the last 30 000 years, the transformation of radiocarbon years into calendar years is based on Bard *et al.* (1993) and Bard (pers. comm.; cf. Hebbeln *et al.* 1994). For the time interval 30 000 to 60 000 years, ages were calculated using mean sedimentation rates between isotope stage boundaries (according to Martinson *et al.* 1987). Hatched areas underline correlation of IRD peaks with cold intervals of the GRIP record. Arrows indicate positive correlation between IRD and magnetic susceptibility peaks. Small numbers (1–17) in the GRIP record indicate interstadials.

the marine record is more complete and therefore more reliable than the terrestrial record for estimating ages of major glacial pulses.

To estimate abundances of IRD and to differentiate between different source areas of the terrigenous (ice-rafted) material, magnetic susceptibility data can be used (e.g. Nowaczyk 1991; Fütterer 1992; Robinson *et al.* 1995). In Fig. 8 magnetic susceptibility values and IRD contents of selected lower slope cores from the four profiles are shown. Most magnetic susceptibility values vary between 50 and 300 (core PS1919), 50 and 200 (cores PS1926 and PS1726) and 100 and 900 10^{-5} SI (core PS1950). At all four cores, minimum values occur in the uppermost oxygen isotope stage 1. This distinct decrease in magnetic susceptibility during the transition from stage 2 to 1 coincides with a major decrease in IRD input (see later). The higher magnetic susceptibility values at the southernmost core PS1950 may reflect a different

source rock mineralogy compared with the northern cores. At core PS1950, the source area of the terrigenous material is most probably the basalt plateau of the southern border of Scoresby Sund (Geikie Plateau; Funder 1989). During the LGM, the Scoresby Sund glaciers transported large amounts of basaltic material characterized by high magnetic susceptibility values to the core location, whereas the source area of the terrigenous material deposited at the northern cores is probably the Mesozoic/Palaeozoic sedimentary rocks of East Greenland.

Comparing IRD and magnetic susceptibility records of the same core show that IRD maxima do not always correspond to high magnetic susceptibility values (Figs 8 and 9). Perhaps this indicates changes in the source areas of the IRD through time. In Fig. 9 the fluctuations in IRD input at core PS1726 are plotted versus calendar years. In these records, the IRD peaks

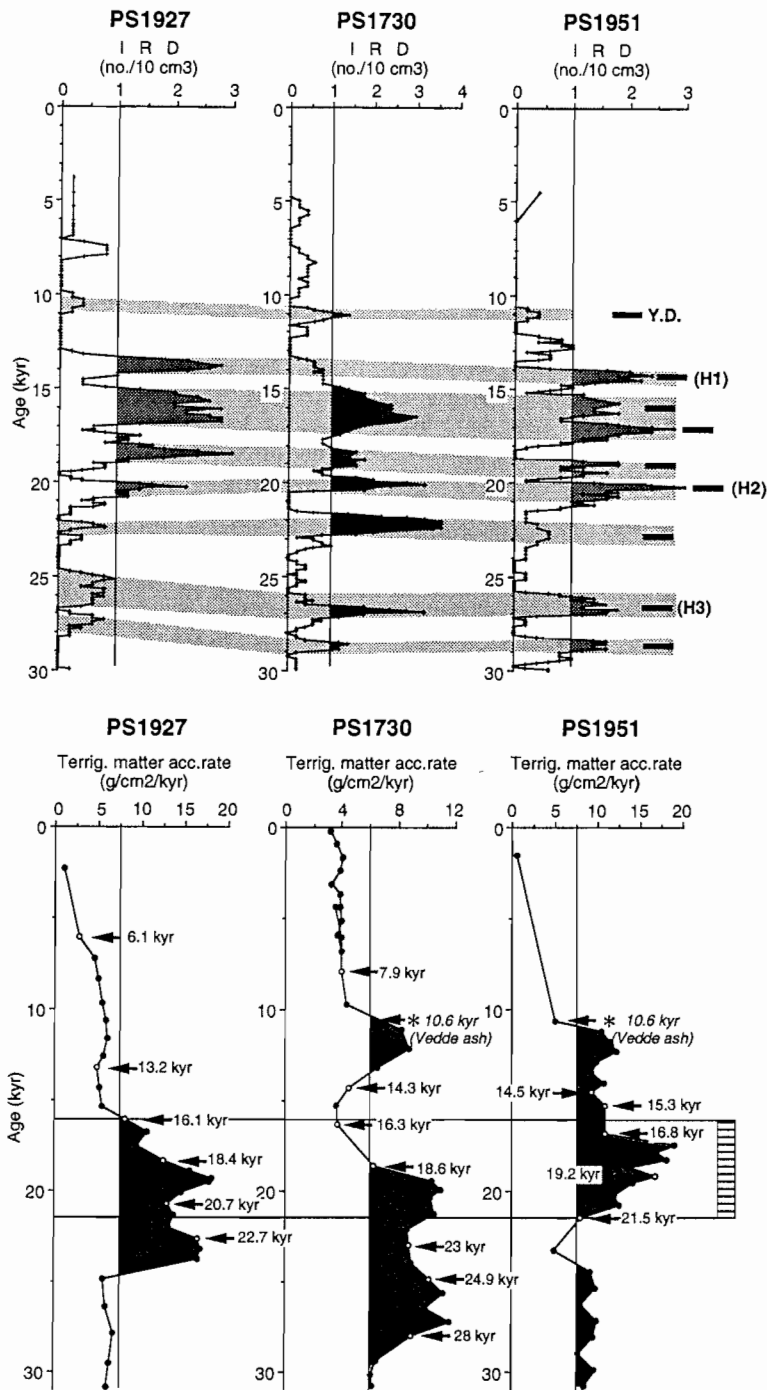


Fig. 10. Amount of IRD and flux rates of terrigenous matter ($\text{g}/\text{cm}^2/\text{ka}$), plotted versus reservoir-corrected radiocarbon ages (cf. Table 2). Black bars at the IRD record indicate major pulses of IRD discharge; Heinrich events (H1, H2 and H3) and the Younger Dryas (YD) event are marked. Hatched bar indicates interval of maximum flux of terrigenous matter, recorded contemporaneously at all three cores.

at about 18, 21, 24, 31 and 48 ka coincide with relatively high magnetic susceptibility values. The IRD maxima at about 16, 38, 44, 52 and 58 ka, on the other hand, do not show any such increased values. This means that the former IRD peaks may contain higher amounts of basaltic material, whereas the latter IRD intervals are relatively enriched in sedimentary rock fragments. It has to be considered, however, that the whole core magnetic susceptibility technique automatically provides a smoothed record and single IRD peaks of a few centimetres in thickness may be not reflected in the magnetic susceptibility record. A more detailed mapping and characterization of the different lithologies at the cores from all other profiles using microscopy and XRD analyses follows to distinguish between local and regional IRD events.

A comparison of the IRD signal off Scoresby Sund and the isotope record from the GRIP Summit Ice Core (Dansgaard *et al.* 1993; Fig. 9) suggests that most of the distinct IRD peaks coincide with intervals of very light isotope values, i.e. times of colder air temperatures over Greenland. In addition, at our study sites, increased iceberg discharges occur more frequently than the Heinrich Events (cf. Bond & Lotti 1995; Fronval *et al.* 1995). The iceberg discharge in the Norwegian Sea from the Fennoscandian Ice Sheet correlates with the GRIP Greenland air temperature record in the same way as our IRD record off Greenland (Fronval *et al.* 1995). Thus our data support the model of these workers that coherent fluctuations in the Fennoscandian and Laurentide/Greenland ice sheets occur on time-scales of a few thousand of years, i.e. distinctly shorter than the Milankovitch orbital cycles.

The last 30 000 years of East Greenland glacial history

In the well-dated cores PS1927, PS1730 and PS1951, changes in IRD discharge are presented in more detail for the last 30 000 years (Fig. 10). Major IRD pulses occur almost contemporaneously at all three cores near 29, 27–26, 23–22, 21–20, 18–17, 16 and 15–14 (radiocarbon) ka. The peaks at 27–26, 21–20, and 15–14 (radiocarbon) ka (or 31–30, 22–21 and 16–15 ka in calendar years; Fig. 9) are correlated with the Heinrich events H3, H2 and H1, respectively. Thus drastic events in iceberg discharge along the East Greenland continental margin recurred at very short intervals of 1000–3000 years, suggesting short-term collapses of the Greenland Ice

Sheet on these time-scales. Short-term fluctuations of IRD deposition on millennial time-scales, i.e. much more frequently than the about 10 000 years associated with Heinrich events, have been described by Bond & Lotti (1995) from their high-resolution studies of North Atlantic deep-sea sediments.

At all three cores, maximum fluxes of (coarse-grained) terrigenous material occur between about 21 and 16 ka BP (Fig. 10). Within this period, the maximum IRD discharges were also recorded (cf. for example, the distinct IRD pulse at deep-sea core PS1922, AMS ^{14}C dated to 18.6 ka; Fig. 4c). The Greenland Ice Sheet probably had its maximum late Weichselian extension and reached the fjord mouth and shelf areas during this period. This event coincides in age and duration with the culmination of the Flakkerhuk stade described in the Jameson Land/Scoresby Sund area (Funder 1989; Funder *et al.* 1994). Large amounts of terrigenous material deposited at the continental margin might have been derived from the inner Scoresby Sund, where all young un lithified sediments were most probably eroded by glaciers (Dowdeswell *et al.* 1991; Uenzelmann-Neben *et al.* 1991; Marienfeld 1992). This late Weichselian East Greenland ice sheet oscillation appears to be in phase with that in the Barents Sea area (Hebbeln *et al.* 1994; Stein *et al.* 1994a).

The most prominent change from the end of the last glacial to the Holocene time (Termination 1) is characterized by a shift in the oxygen isotope records towards lighter values and by a decrease in the amount of IRD (Figs 4–7). This lowered ice rafting from Greenland near 15–14 ka is earlier than the rapid glacial retreat on Svalbard around 13–12.5 ka (e.g. Svendsen & Mangerud 1992).

The increased flux rates of terrigenous material at about 11 ka, which coincide with slightly increased abundances of IRD (Fig. 10), correspond to the Younger Dryas cooling event (e.g. Duplessy *et al.* 1981; Fairbanks 1989; Andrews *et al.* 1990; Kennett 1990). At that time, i.e. after the recession of glaciers that followed the Flakkerhuk glaciation, the East Greenland glaciers advanced again, however, without reaching the outer fjords/shelf ('Milne Land stade'; Funder 1989). These re-advanced glaciers may have caused the increase in IRD discharge near 11 ka.

Minor amounts of IRD were deposited at all core sites during the Holocene (Figs 4–7). Most of the material transported by icebergs was already discharged and deposited in the fjords, as shown for the Scoresby Sund fjord system (Marienfeld 1992; Stein *et al.* 1993).

Conclusions

The results of our detailed sedimentological investigations of sediment cores from the East Greenland continental margin can be summarized as follows.

- (1) The sedimentary records give important information about the East Greenland glacial history during the last 190 ka. Most of the oxygen isotope curves resemble the global isotope record, with some excursions to lighter values representing local/regional meltwater events.
- (2) According to the amount of IRD, numerous major pulses of glacial activity and supply of terrigenous material by glacio-marine processes occurred during the last 190 ka. The correlation between IRD peaks and magnetic susceptibility suggests changes in the composition of IRD in time and space, reflecting iceberg discharge from different source areas. This conclusion, however, has to be proved by further microscopic and XRD analyses of the terrigenous material.
- (3) A comparison of the IRD signal off Scoresby Sund and the oxygen isotope records from the GRIP Summit Ice Core suggests that most of the distinct IRD peaks coincide with times of colder air temperatures over Greenland.
- (4) The events in iceberg discharge along the East Greenland continental margin recurred at very short intervals of 1000–3000 years. Rapid collapses of the Greenland Ice Sheet occur on millennial time-scales, i.e. more frequently than the 5000–10 000 years frequency associated with Heinrich events. Furthermore, our data support coherent fluctuations in the Fennoscandian/Barents Sea and Laurentide/Greenland ice sheets.
- (5) The maximum flux of terrigenous (coarse-grained) material recorded at about 21–16 ka indicates the maximum late Weichselian extension of the East Greenland Ice Sheet. This event coincides in age and duration with the culmination of the Flakkerhuk stade described in the Jameson Land/Scoresby Sund area.
- (6) The increased flux rates of terrigenous material and slightly increased abundances of IRD at about 11 ka correspond to the Younger Dryas cooling event or Milne Land stade glacial advance.

For technical assistance and discussion of data, we sincerely thank G. Meyer, H. Röben, N. Scheele and M. Seebeck. The AMS ^{14}C datings were performed by J. Heinemeier, Institute of Physics and Astronomy,

Aarhus University, Denmark. The captain and the crew of R.V. *Polarstern* are gratefully acknowledged for co-operation during the expeditions ARK-V/3 and ARK-VII/3. We thank A. Geirsdóttir and F. R. Hall for their numerous constructive comments for improvement of the manuscript. This is contribution No. 1025 of the Alfred Wegener Institute for Polar and Marine Research.

References

- ANDREWS, J. T. & TEDESCO, K. 1992. Detrital carbonate-rich sediments, northwestern Labrador Sea: implications for ice-sheet dynamics and iceberg rafting (Heinrich) events in the North Atlantic. *Geology*, **20**, 1087–1090.
- , EVANS, L. W., WILLIAMS, K. M., BRIGGS, W. M., ERLKENKEUSER, H., HARDY, I. & JULL, A. J. T. 1990. Cryosphere-ocean interactions at the margin of the Laurentide Ice Sheet during the Younger Dryas Chron: southeastern Baffin shelf, Northwest Territories. *Paleoceanography*, **5**, 921–935.
- BARD, E., ARNOLD, M., FAIRBANKS, R., & HAMELIN, B. 1993. ^{230}Th – ^{234}Cl and ^{14}C ages obtained by mass spectrometry in corals. *Radiocarbon*, **35**, 191–199.
- BAUMANN, K.-H., LACKSCHEWITZ, K. S., ERLKENKEUSER, H., HENRICH, R. & JÜNGER, B. 1993. Late Quaternary calcium carbonate sedimentation and terrigenous input along the East Greenland continental margin. *Marine Geology*, **114**, 13–36.
- BIRGISDÓTTIR, L. 1991. Die paläo-ozeanographische Entwicklung der Islandsee in der letzten 550,000 Jahre. *Berichte SFB 313, Universität Kiel*, **34**.
- BOND, G. C. & LOTTI, R. 1995. Iceberg discharges into the North Atlantic on millennial time scales during the last glaciation. *Science*, **267**, 1005–1010.
- , HEINRICH, H. & 12 others 1992. Evidence for massive discharges of icebergs into the North Atlantic ocean during the last glacial period. *Nature*, **360**, 245–249.
- BROECKER, W., BOND, G., KLASS, M., CLARK, E. & MCMANUS, J. 1992. Origin of the northern Atlantic's Heinrich events. *Climate Dynamics*, **6**, 265–273.
- CHAPPELL, J. & SHACKLETON, N. J. 1986. Oxygen isotopes and sea level. *Nature*, **324**, 137–140.
- DANSGAARD, W., JOHNSEN, S. J., & 9 others 1993. Evidence for general instability of past climate from a 250-kyr ice-core record. *Nature*, **364**, 218–220.
- DOWDESWELL, J. A., VILLINGER, H., WHITTINGTON, R. J. & MARIENFELD, P. 1991. The Quaternary marine record in the Scoresby Sund fjord system, East Greenland: preliminary results and interpretation. In: MÖLLER P. *et al.* (eds) *The Last Interglacial-Glacial Cycle: Jameson Land and Scoresby Sund, East Greenland*. LundQua Report Series, **33**, 149–155.
- DUPLESSY, J. C., DELIBRIAS, G., TURON, J. L., PUJOL, C. & DUPRAT, J. 1981. Deglacial warming of the northeastern Atlantic Ocean: correlation with the paleoclimatic evolution of the European continent. *Palaeogeography, Palaeoclimatology, Palaeoecology*, **35**, 121–144.

- , LABEYRIE, L., JUILLET-LECLERC, A., MAITRE, F., DUPRAT, J. & SARNTHEIN, M. 1991. Surface salinity reconstruction of the North Atlantic Ocean during the last glacial maximum. *Oceanologica Acta*, **14**, 311–324.
- ELVERHØI, A. & DOWDESWELL, J. A. 1991. Polar North Atlantic Margins (PONAM). *ESF – Communications*, **25**, 16–17.
- FAIRBANKS, R. G. 1989. A 17,000-year glacio-eustatic sea level record: influence of glacial melting rates on the Younger Dryas event and deep-ocean circulation. *Nature*, **342**, 637–642.
- FRONVAL, T., JANSEN, E., BLOEMENDAL, J. & JOHNSEN, S. 1995. Oceanic evidence for coherent fluctuations in Fennoscandian and Laurentide ice sheets on millennium timescales. *Nature*, **374**, 443–446.
- FUNDER, S. 1984. Chronology of the last interglacial/glacial cycle in Greenland: first approximation. In: MAHANEY W. C. (ed.) *Correlation of Quaternary chronologies*. Geo Books, Norwich, 261–279.
- 1989. Quaternary geology of the ice-free areas and adjacent shelves of Greenland. In: FULTON, R. J. (ed.) *Quaternary Geology of Canada and Greenland*. Geological Survey of Canada, Geology of Canada, **1** (also Geological Society of America, The Geology of the North America, K-1), 743–792.
- , HJORT, C., & LANDVIK, J. Y. 1994. The last glacial cycle in East Greenland, an overview. *Boreas*, **23**, 283–293.
- FÜTTERER, D. K. 1992. ARCTIC'91: the Expedition ARK-VIII/3 of RV 'Polarstern' in 1991. *Berichte zur Polarsternforschung*, **107**.
- GARD, G. & BACKMAN, J. 1990. Synthesis of Arctic and subarctic coccolith biochronology and history of North Atlantic Drift Water influx during the last 500,000 years. In: BLEIL, U. & THIEDE, J. (eds) *Geological History of the Polar Oceans: Arctic Versus Antarctic*. Nato ASI Series C, Kluwer Academic, Dordrecht, **308**, 539–576.
- GORSHKOV, S. G. 1983. *World Ocean Atlas*. Vol. 3. *Arctic Ocean*. Pergamon, Oxford.
- GROBE, H. 1987. A simple method for the determination of ice-rafted debris in sediment cores. *Polarforschung*, **57**, 123–126.
- HEBBELN, D., DOKKEN, T., ANDERSEN, E. S., HALD, M., & ELVERHØI, A. 1994. Moisture supply for northern ice-sheet growth during the Last Glacial Maximum. *Nature*, **370**, 357–360.
- HEINRICH, H. 1988. Origin and consequences of cyclic ice rafting in the northeast Atlantic Ocean during the past 130,000 years. *Quaternary Research*, **29**, 142–152.
- HEINRICH, R., KASSENS, H., VOGELSANG, E. & THIEDE, J. 1989. Sedimentary facies of glacial-interglacial cycles in the Norwegian Sea during the last 350 ka. *Marine Geology*, **86**, 283–319.
- HJORT, C. 1981. A glacial chronology for the northern East Greenland. *Boreas*, **10**, 259–274.
- ISRAELSON, C., FUNDER, S., & KELLY, M. 1994. The Aucellaelv stade at Aucellaelv, the first Weichselian glacier advance in scoresby Sund, East Greenland. *Boreas*, **23**, 424–431.
- JONES, G. A. & KEIGWIN, L.D. 1988. Evidence from Fram Strait (78°N) for early deglaciation. *Nature*, **336**, 56–59.
- JÜNGER, B. 1993. *Tiefenwassererneuerung in der Grnlandsee während der letzten 340 000 Jahre*. PhD Dissertation, Universität Kiel.
- KENNETT, J. P. 1990. The Younger Dryas cooling event: an introduction. *Paleoceanography*, **5**, 891–896.
- KOÇKARPUZ, N. & JANSEN, E. 1992. A high-resolution diatom record of the last deglaciation from the SE Norwegian Sea: documentation of rapid climatic changes. *Paleoceanography*, **7**, 499–520.
- LACKSCHEWITZ, K. S. 1991. Sedimentationsprozesse am aktiven mittelozeanischen Kolbeinsey Rücken, nördlich von Island. *Geomar Report*, **9**.
- MANGERUD, J., LIE, S. E., FURNES, H. & KRISTIANSEN, I. L. 1984. A Younger Dryas ash bed in Western Norway, and its possible correlations with tephra in cores from the Norwegian Sea and the North Atlantic. *Quaternary Research*, **21**, 85–104.
- MARIENFELD, P. 1992. Postglacial sedimentary history of Scoresby Sund, East Greenland. *Polarforschung*, **60**, 181–195.
- MARTINSON, D. G., PISIAS, N. G., HAYS, J. D., IMBRIE, J., MOORE, T. C., & SHACKLETON, N. J. 1987. Age dating and the orbital theory of ice ages: development of high-resolution 0 to 300,000-year chronostratigraphy. *Quaternary Research*, **27**, 1–29.
- MIENERT, J., ANDREWS, J. T. & MILLIMAN, J. D. 1992. The East Greenland continental margin (65°N) since the last deglaciation: changes in seafloor properties and ocean circulation. *Marine Geology*, **106**, 217–238.
- MØLLER, P., HJORT, C., ADRIELSSON, L. & SALVIGSEN, O. 1994. Glacial history of interior Jameson Land, East Greenland. *Boreas*, **23**, 320–348.
- , HJORT, C. & INGOLFSSON, O. 1991. The last interglacial/glacial cycle: preliminary report on the PONAM fieldwork in Jameson Land and Scoresby Sund, East Greenland. *Lundqua Rep*, **33**.
- NAM, S.-I. 1996. *Late Quaternary glacial/interglacial changes in paleoclimate and paleoceanographic circulation along the East Greenland continental margin*. PhD Thesis, Bremen University.
- , STEIN, R., GROBE, H. & HUBBERTEN, H. 1995. Late Quaternary glacial/interglacial changes in sediment composition at the East Greenland continental margin and their paleoceanographic implications. *Marine Geology*, **122**, 243–262.
- NOWACZYK, N. R. 1991. Hochauflösende Magnetostatigraphie spätquartärer Sedimente arktischer Meeresgebiete. *Berichte zur Polarforschung*, **78**.
- ROBINSON, S. G., MASLIN, M. A. & MCCAVE, I. N. 1995. Magnetic susceptibility variations in late Pleistocene deep-sea sediments of the N.E. Atlantic: implications for ice-rafting and paleocirculation at the last Glacial Maximum. *Paleoceanography*, **10**, 221–250.
- RUDDIMAN, W. F. 1977. North Atlantic ice-rafting: a major change at 75,000 years before the present. *Science*, **196**, 1208–1211.

- SARNTHEIN, M., JANSEN, E. & 7 others 1992. $\delta^{18}\text{O}$ time-slice reconstruction of meltwater anomalies at Termination I in the North Atlantic between 50 and 80° N. In: BARD, E. & BROECKER, W. S. (eds) *The Last Deglaciation: Absolute and Radiocarbon Chronologies*. NATO ASI Series, **12**, 183–200.
- SEJRUP, H. P., SJØHOLM, J., FURNES, H., BEYER, I., EIDE, L., JANSEN, E. & MANGERUD, J. 1989. Quaternary tephrochronology on the Iceland Plateau, north of Iceland. *Journal of Quaternary Science*, **4**, 109–114.
- SHACKLETON, N. J. 1987. Oxygen isotopes, ice volume and sea level. *Quaternary Science Reviews*, **6**, 183–190.
- & OPDYKE, N. D. 1973. Oxygen isotope and paleomagnetic stratigraphy of equatorial Pacific Core V28–238: oxygen isotope temperatures and ice volume on a 105 year and 106 year scale. *Quaternary Research*, **3**, 39–55.
- , BACKMAN, J. & 7 others 1984. Oxygen isotope calibration of the onset of ice-rafting and history of glaciation in the North Atlantic region. *Nature*, **307**, 620–623.
- SPIELHAGEN, R. F. 1991. Die Eisdrift in der Framstrasse während der letzten 200 000 Jahre. *GEOMAR Report*, **4**.
- STEIN, R., GROBE, H., HUBBERTEN, H., MARIENFELD, P. & NAM, S. 1993. Latest Pleistocene to Holocene changes in glaciomarine sedimentation in Scoresby Sund and along the adjacent East Greenland Continental Margin: Preliminary results. *Geo-Marine Letters*, **13**, 9–16.
- , NAM, S.-I., SCHUBERT, C., VOGT, C., FÜTTERER, D. & HEINEMEIER, J. 1994a. The last deglaciation event in the eastern central Arctic Ocean. *Science*, **264**, 692–696.
- , SCHUBERT, C., VOGT, C., & FÜTTERER, D. K. 1994b. Stable isotope stratigraphy, sedimentation rates, and salinity changes in the latest Pleistocene to Holocene central Arctic Ocean. *Marine Geology*, **119**, 333–355.
- STREETER, S. S., BELANGER, P. E., KELLOGG, T. B. & J. C. DUPLESSY 1982. Late Pleistocene paleo-oceanography of the Norwegian-Greenland Sea: benthic foraminiferal evidence. *Quaternary Research*, **18**, 72–90.
- SVENDSEN, J. I. & MANGERUD, J. 1992. Paleoclimatic inferences from glacial fluctuations on Svalbard during the last 20,000 years. *Climate Dynamics*, **6**, 213–220.
- UENZELMANN-NEBEN, G., JOKAT, W. & VANNESTE, K. 1991. Quaternary sediments in Scoresby Sund, East Greenland: their distribution as revealed by reflection seismic data. *Lundqua Report*, **33**, 139–148.
- VAN ANDEL, T. H., HEATH, G. R. & MOORE, T. C. 1975. *Cenozoic History and Paleooceanography of the Central Equatorial Pacific*. Memoir of the Geological Society of America, **143**.
- VOGELSANG, E. 1990. Paläo-Ozeanographie des Europäischen Nordmeeres an Hand stabiler Kohlenstoff- und Sauerstoffisotope. *Berichte SFB 313, Universität Kiel*, **23**.
- WILLIAMS, K. M. 1993. Ice sheet and ocean interactions, margin of the east Greenland ice sheet (14 ka to Present): diatom evidence. *Paleoceanography*, **8**, 69–83.